Electronic Supplementary Material (ESI) for Energy Advances.

Supporting Information:

Strategies to Improve the Mechanical Robustness of Metal Halide Perovskite Solar Cells

Muzhi Li[1], Samuel Johnson[2], Lidon Gil-Escrig[3], Maayan Sohmer[4], Carlos A. Figueroa Morales[5], Hongki Kim[5], Siraj Sidhik[6], Aditya Mohite[6], Xiwen Gong[5], Lioz Etgar[4], Henk J. Bolink[3], Axel Palmstrom[7], Michael D. McGehee[2] and Nicholas Rolston[1]

[1]Arizona State University, Tempe, Arizona, 85281, U.S.A.
[2]University of Colorado Boulder, Boulder, Colorado, 80309, U.S.A.
[3]University of Valencia, Valencia, 46003, Spain
[4]The Institute of Chemistry, The Center for Nanoscience and Nanotechnology, Casali Center for Applied Chemistry, The Hebrew University of Jerusalem, Jerusalem, 91904, Israel
[5]University of Michigan, Ann Arbor, Michigan, 48109, U.S.A.
[6]Rice University, Houston, Texas, 77251, U.S.A.
[7]National Renewable Energy Laboratory, Golden, Colorado, 80401, U.S.A.

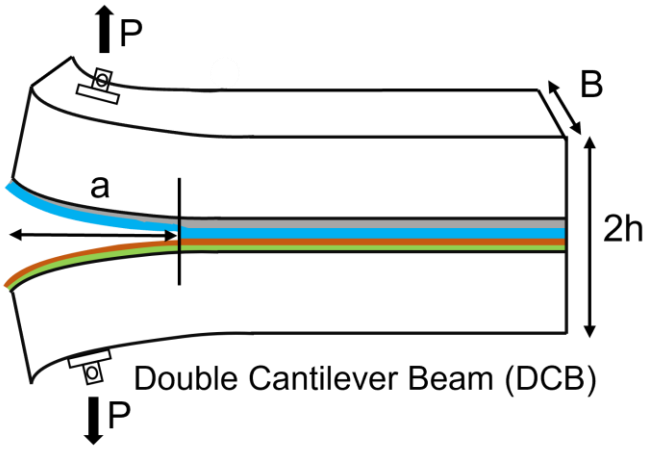

$$G_c = \frac{12 P_c^2 a^2}{B^2 E' h^3}\left(1 + 0.64\frac{h}{a}\right)^2$$

P_C – critical load
a – crack length
B – specimen width
h – half-thickness
E' – plane strain Young's modulus of substrate

Fig. S1 The schematic diagram of DCB specimen with G_c formula

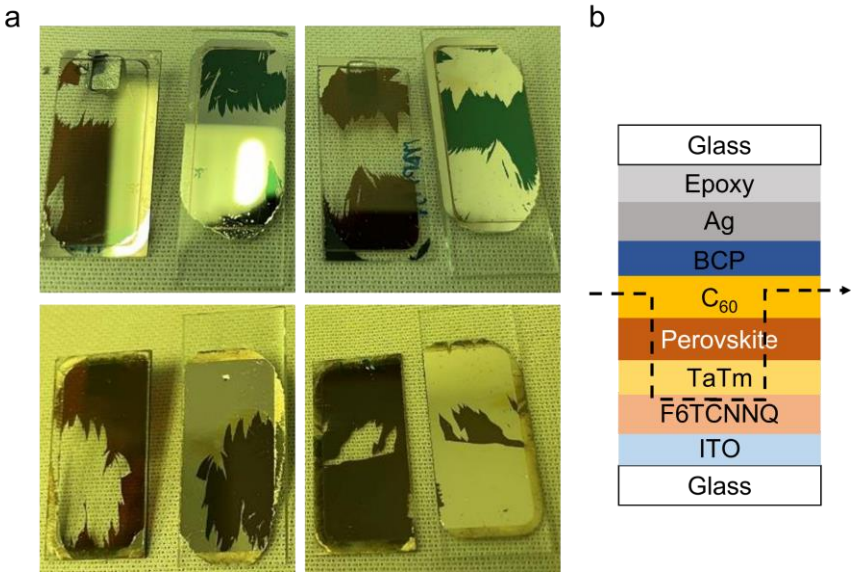

Fig. S2 (a) The optical images of the fractured p-i-n DCB samples. (b) Sample structure and fracture path. The perovskite was not observed simultaneously at the same spot on both glass substrates, indicating that the P and N sections are the most fragile components in the device.

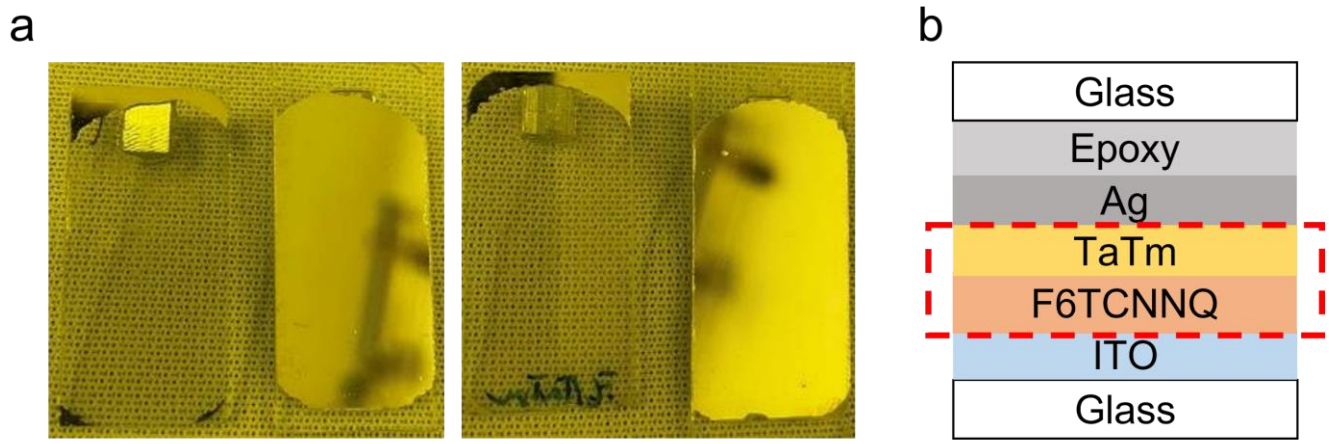

Fig. S3 (a) The optical images of fractured HTMs DCB samples (b) The sample structure and most fragile section (indicated by the red dashed rectangle)

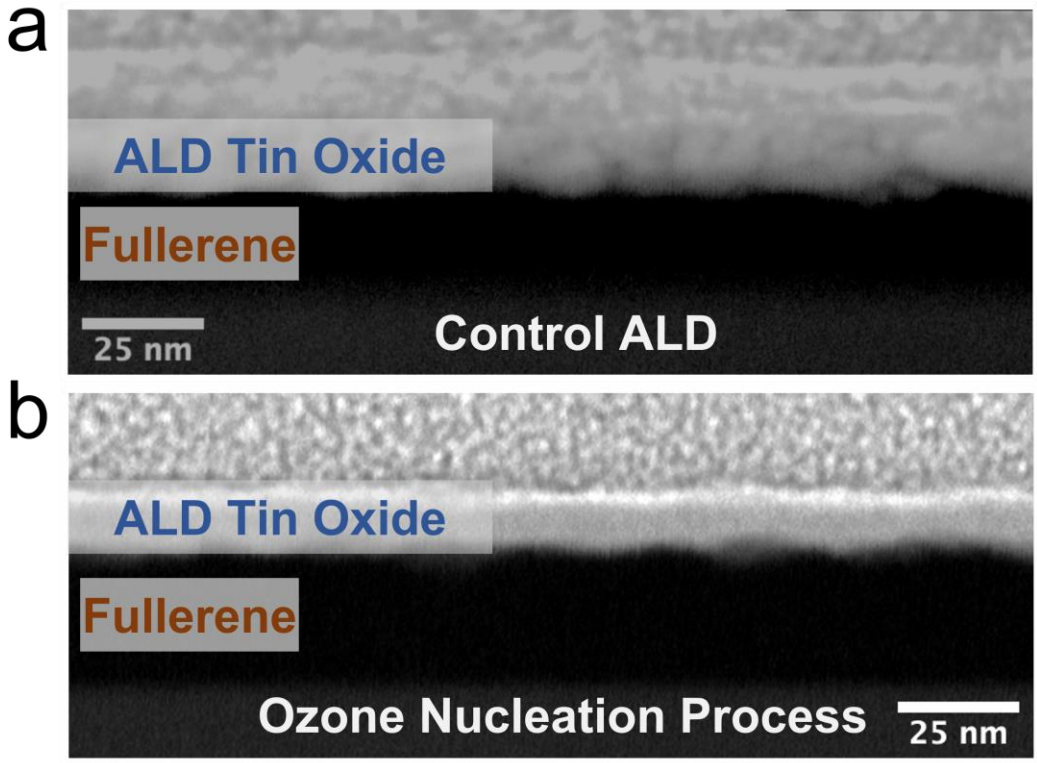

Fig. S4 The cross-sectional STEM images of the interface of ALD-SnO_x and C_{60} (a) without and (b) with ozone nucleation process

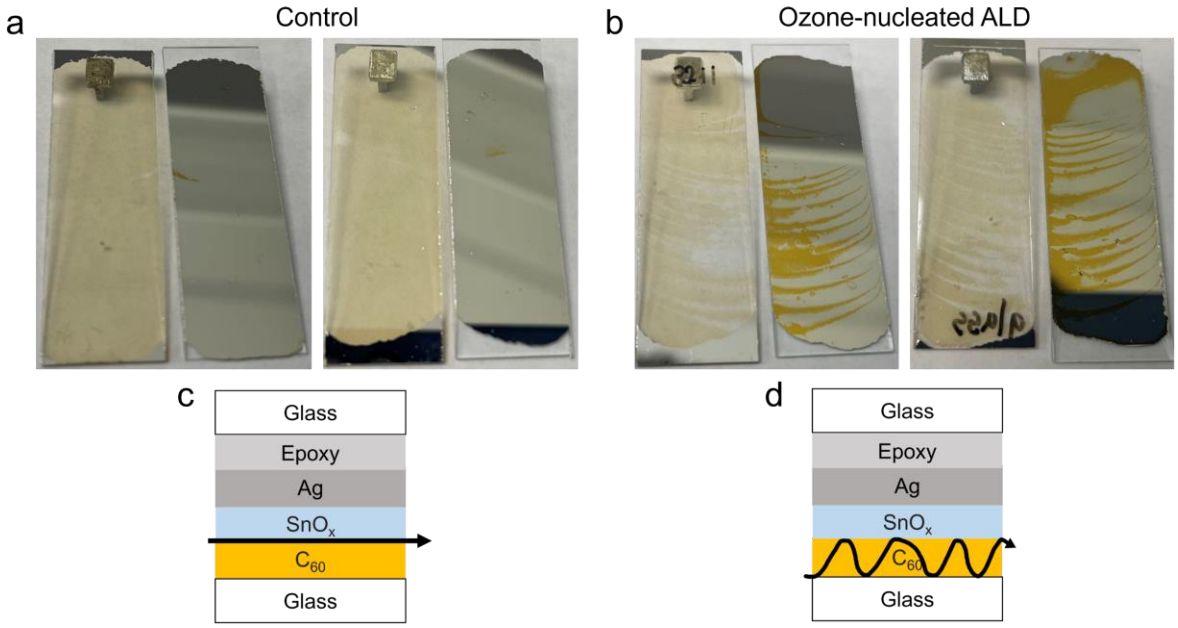

Fig. S5 The optical images of the fractured (a) control ALD-SnO_x and (b) ozone-nucleated ALD-SnO_x samples. (c) and (d) show the sample structure and fracture paths.

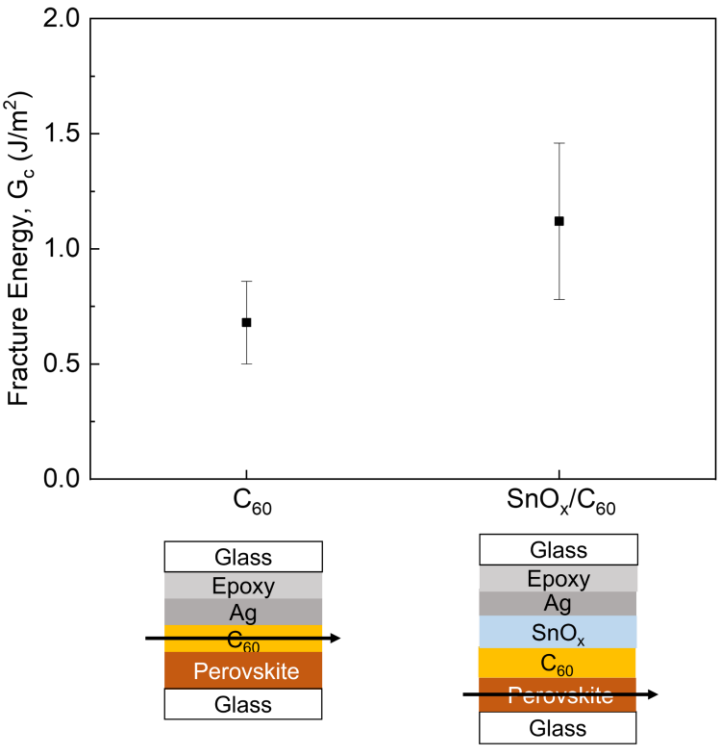

Fig. S6 The measured G_c values and fracture paths of samples with and without SnO_x.

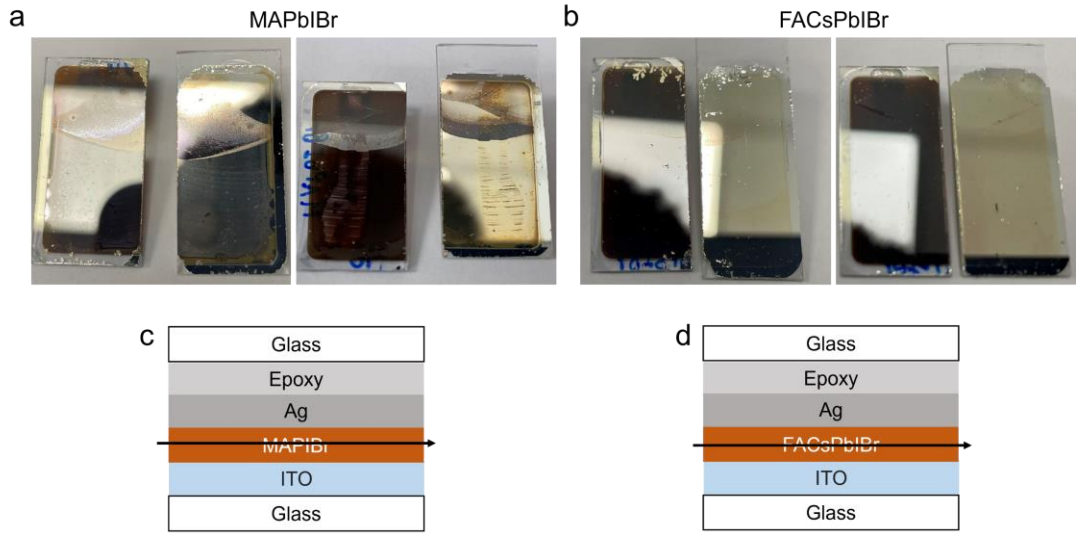

Fig. S7 The optical images of fractured (a) $MAPb(I_{0.9}Br_{0.1})_3$ and (b) $FA_{0.74}Cs_{0.26}Pb(I_{0.86}Br_{0.14})_3$ DCB samples. (c) and (d) show the sample structures and fracture paths.

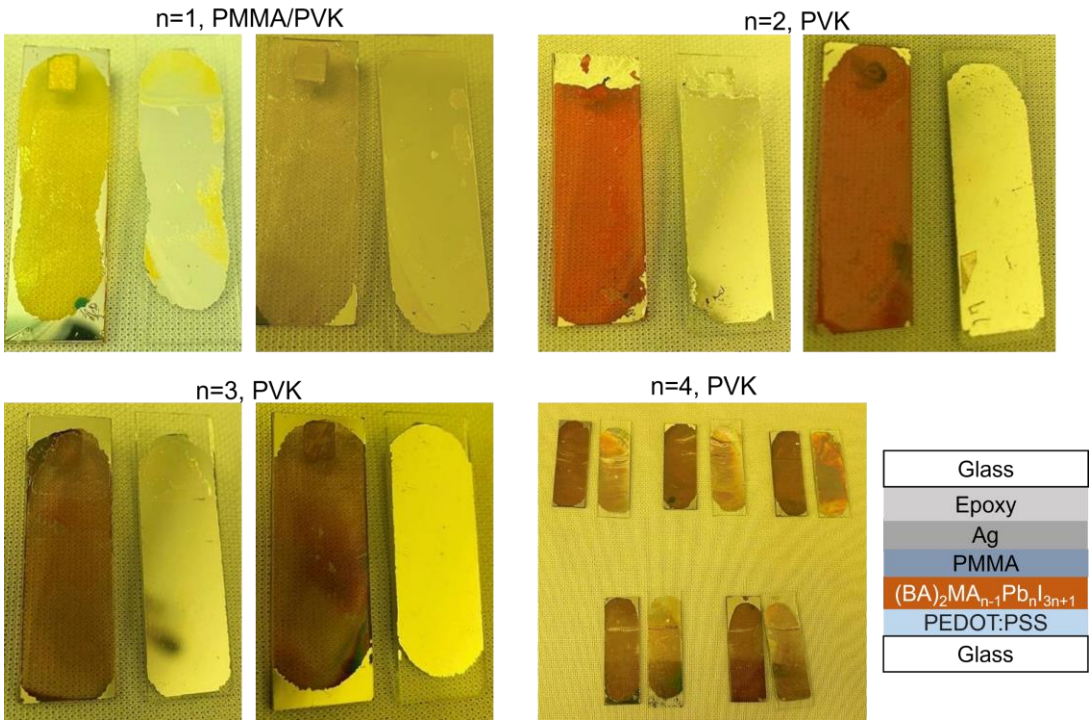

Fig. S8 The optical images of fractured BA-based 2D perovskite DCB samples with different n-value and fracture paths.

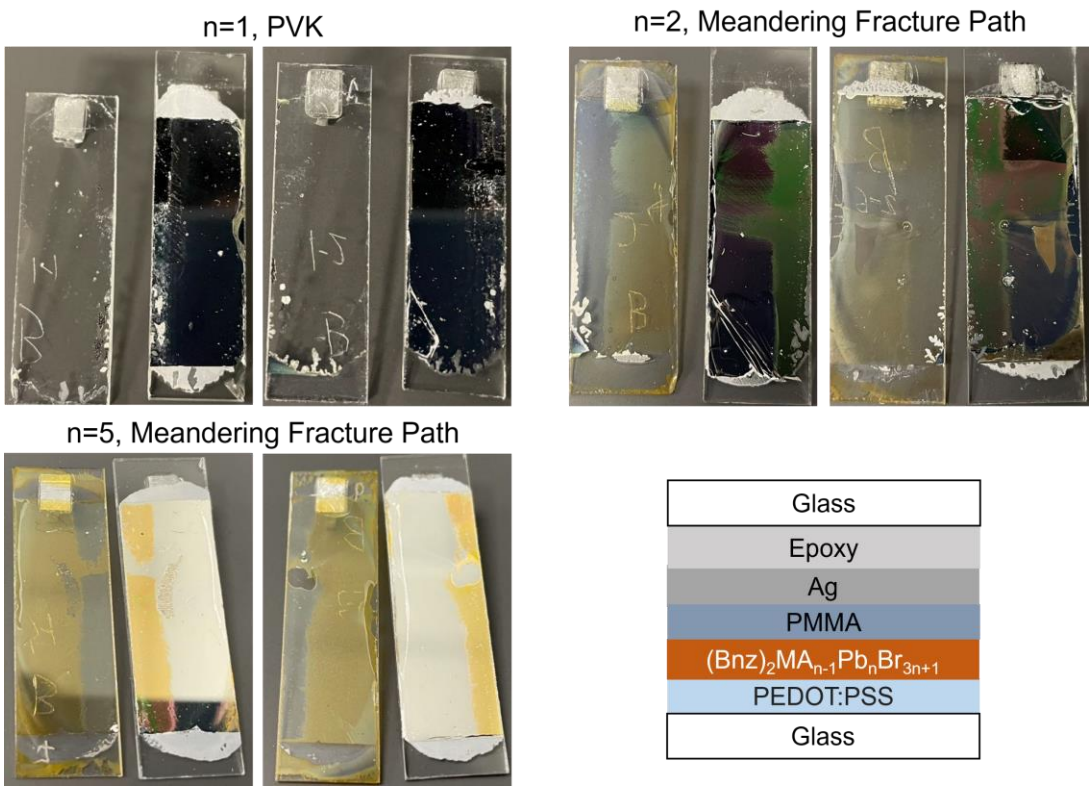

Fig. S9 The optical images of fractured Bnz-based 2D perovskite DCB samples with different n-value and fracture paths.

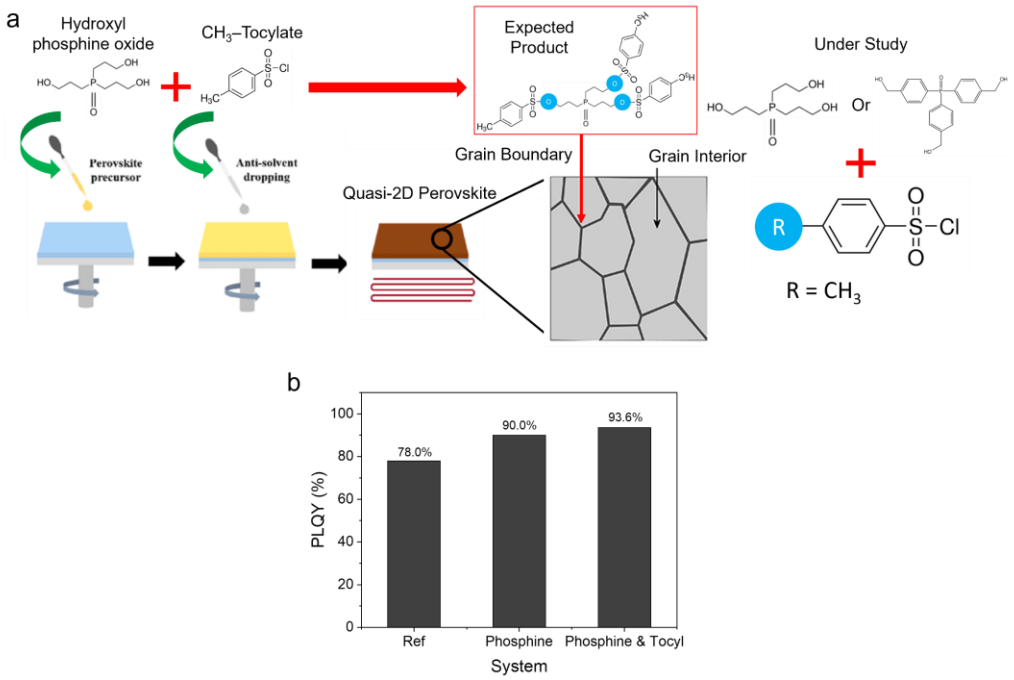

Fig. S10 (a) The schematic diagrams of the incorporation process of the additives in perovskite. (b) Photoluminescence quantum yield of the reference sample and samples with additives.

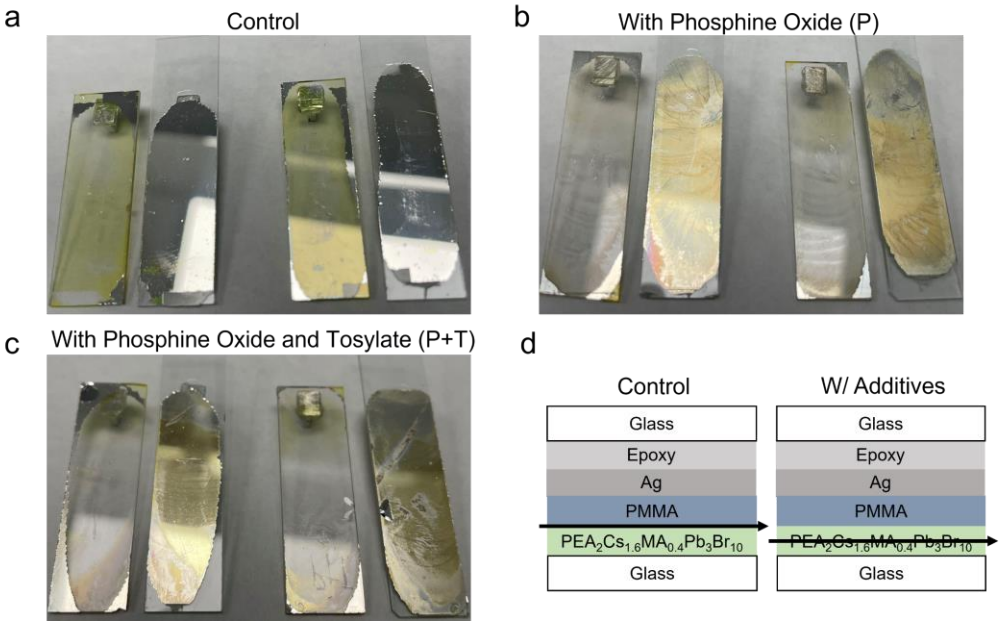

Fig. S11 The optical images of the fractured (a) control samples and samples with (b) phosphine oxide additive and (c) phosphine oxide/tocylate additives. (d) The sample structures and fracture paths.

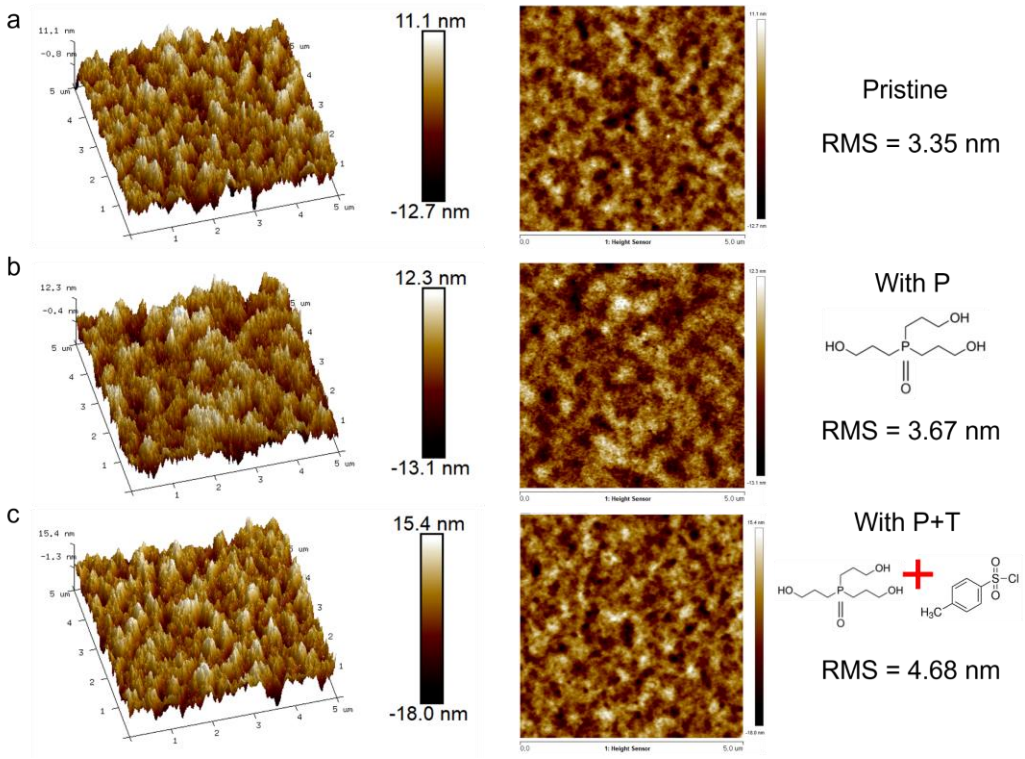

Fig. S12 The atomic force microscopy height images featuring the topography of the perovskite films (a) without additives, (b) with phosphine oxide additive, and (c) with phosphine oxide and tocylate additives.